Polymorphism and chiral expression in two-dimensional subphthalocyanine crystals on Au(111)†

Nan Jiang,[a] Yeliang Wang,[a] Qi Liu,[a] Yuyang Zhang,[a] Zhitao Deng,[a] Karl-Heinz Ernst*[b] and Hong-Jun Gao*[a]

Received 4th September 2009, Accepted 11th November 2009
First published as an Advance Article on the web 10th December 2009
DOI: 10.1039/b918278k

The adsorption of subphthalocyanine (SubPc) on the Au(111) surface has been studied by scanning tunnelling microscopy (STM). Depending on coverage and deposition temperature, four different phases have been observed, of which two are coexisting. Spontaneous symmetry breaking inducing mirror domains is observed for all structures. Supramolecular chirality is expressed at different levels and length scale. Our detailed STM study allows conclusions on the origin of polymorphism due to changing coverage and temperature.

Introduction

Porphyrins and phthalocyanines (Pc) with various metal atoms at the centres have attracted special interest over the past two decades as important compounds for organic electronic devices such as organic light-emitting diodes (OLED), thin film transistors (OFETs), and photovoltaic devices.[1–6] In particular the physical chemistry at electrode interfaces of such devices is important for their performance.[7] Therefore, the geometric and the electronic structures of metal-Pc (MPc) molecules deposited on metallic surfaces have been investigated in detail with different methods, including high spatial resolution by scanning tunnelling microscopy (STM).[8]

Adsorption of bowl-shaped molecules has become in particular interesting for studying fundamental symmetry mismatching,[9–12] phase transitions,[13,14] and further surface modification with C_{60}.[15] The subphthalocyanine (SubPc, Fig. 1a) is a special member in the family of metallic phthalocyanines because of its bowl geometry.[16] It has only three isoindolyl groups instead of four in the common MPc. The central boron atom is sp^3-coordinated to all isoindolyl groups and to the axial chlorine atom, which leads to a bowl-shaped molecular frame. Since the first synthesis by Meller and Ossko in 1972,[17] SubPc is still the only known threefold symmetric phthalocyanine. It serves as starting material for synthesis of MPc derivates and often appears as impurity in MPcs. Pure SubPc adsorption and growth has been studied previously.[18–22] On Ag(111) SubPc was found to adsorb with the bowl opening pointing away from the surface.[20] The codeposition with C_{60} on Ag(111) has also been investigated by Jung and coworkers.[23] Due to the high mobility for SubPc on Au(111) at room temperature, Mannsfeld *et al.* reported an ordered structure for the monolayer at saturation.[22] Here we report coverage dependent polymorphism in self-assembled SubPc monolayers on Au(111) investigated by STM at cryogenic temperatures. All structures form mirror domains and exhibit different forms of chiral expression.

Experimental details

Experiments have been performed in an ultrahigh vacuum (UHV) system (base pressure in the range of 10^{-10} mbar) equipped with a low-temperature STM system (Omicron Nanotechnology GmbH) and standard UHV crystal preparation facilities. The Au(111) single crystal (MaTeK, 99.999% purity) was prepared by repeated cycles of Ar ion sputtering and annealing at 700 K. The bare Au(111) surface was characterized by atomic resolution STM for determining the surface orientation. Commercially available SubPc (chloro [subphthalocyaninato]-boron(III), 99% purity, Sigma-Aldrich) was deposited onto the Au(111) surface by molecular beam epitaxy at 500 K, with the Au sample held at room temperature (RT). Low energy electron diffraction (LEED) patterns were recorded with a CCD camera from the back-view LEED optics. The STM measurements were performed at 77 K. The tungsten STM tips had been electrochemically etched in a 2 M NaOH solution. All STM images have been taken in constant-current mode. Global coverages were estimated from many different STM images acquired for the same sample at different areas.

Results and discussion

Depending on coverage and deposition temperature, four different complex structures have been observed at 77 K in STM: a honeycomb structure, a diamond structure, an 'intermediate' structure, which combines packing motifs of diamond and honeycomb, and finally a hexagonal close-packed (hcp) structure.

[a] *Institute of Physics, Chinese Academy of Sciences, Beijing 100190, PR China. E-mail: hjgao@iphy.ac.cn; Fax: +86 1062556598; Tel: +86 10 2648035*
[b] *Nanoscale Materials Science Laboratory, Empa-Swiss Federal Laboratories for Materials Research (EMPA), Überlandstrasse 129, CH-8600 Dübendorf, Switzerland E-mail: karl-heinz.ernst@empa.ch; Fax: +41 448234034; Tel: +41 448234363*

† Electronic supplementary information (ESI) available: Long range STM images and choice of unit cells for the different structure models. See DOI: 10.1039/b918278k

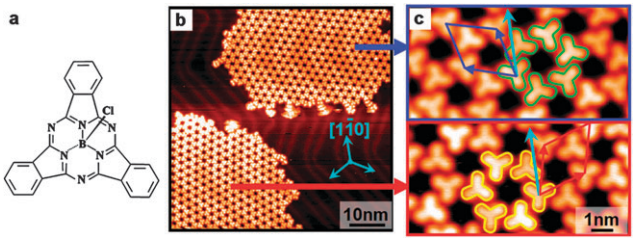

Fig. 1 (a) Chemical structure of SubPC. (b) A large-scale STM image of SubPc islands showing the honeycomb pattern. (c) Details from the two mirror domains shown in (b). Unit cells are indicated in blue and red, respectively. The cyan arrows indicate the closed-packed crystallographic directions of the Au (111) substrate. STM parameters: $U = -2.0$ V, $I = 60$ pA.

Honycomb structure—low global coverage

Fig. 1b shows the STM image obtained at the initial growth stage. Well-ordered two-dimensional (2D) islands on the terraces of the Au(111) substrate are observed, which implies that there is appreciable mobility at the surface until islands nucleate and grow upon cooling. Individual molecules are not observed in the STM images. The molecules are assembled in a 2D quasi-hexagonal honeycomb pattern. Corresponding well to the molecular C_{3v} symmetry, individual SubPc molecules are imaged as three-spoke entities in high-resolution STM images (Fig. 1c). Two mirror domains are observed, both showing the honeycomb pattern, but with opposite expression of chirality.[24] That is, the orientation of the adlattice is tilted clockwise (CW) or counterclockwise (CCW), *i.e.*, by $\pm 15^\circ \pm 1^\circ$ with respect to the [1$\bar{1}$0] substrate direction (Fig. 1c, cyan arrow). In addition, six molecules are geared in a left-handed or right-handed wheel fashion. The unit cell vectors, marked by blue and red arrows, respectively, are 23.0 Å long, leading to a packing density of 0.44 molecules nm^{-2}, ($\theta = 0.032$ molecules per Au substrate atom). The shortest intermolecular distance measured from the STM images is 15.0 ± 1.0 Å.

A tentative structure model of the honeycomb-structure is presented in Fig. 2a. The molecular orientations with respect to the underlying Au(111) are also shown. The phenylene rings of SubPc molecules are adjacent to each other. Since the honeycomb structure nucleates and grows at low coverage, attractive interactions are at work, and the structure forms until repulsive interactions—probably from the hydrogen atoms facing each other from opposite phenylene rings—counter-balance the attraction. This adsorption behaviour is quite different to the situation reported for planar MPc molecules. FePc molecules, for example, adsorb on the Au(111) surface dispersedly at low coverage, which suggests a repulsive interaction among FePc molecules.[25] Such repulsion is ascribed to the dipole interaction that originates from a strong charge transfer from the Au substrate to the metal centres of MPc. A similar observation has been made also for SnPc on Ag(111).[26] For the SubPc case, however, the net dipole should be decreased since intrinsic dipole and the induced dipole have opposite polarity. Thus, unlike the strong interaction between the Fe metal centre of FePc and the Au(111) substrate, the driving force for the well-ordered aggregated patterns of SubPc molecules can easily

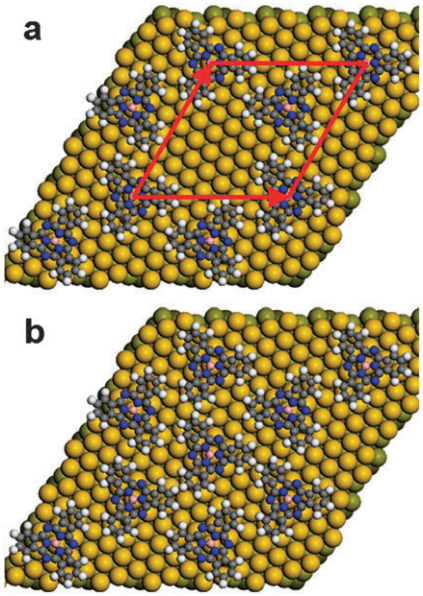

Fig. 2 (a) Model for the honeycomb structure. The unit cell is indicated in red. The chlorine atom has been placed on top of a gold atom. The two molecules in the unit cell are rotated by 60° with respect to each other. (b) Placing an additional molecule into the void in the centre of the hexamer leads to substantial steric constraint between the H-atoms of phenylene rings.

be ascribed to an intermolecular static electronic attraction rather than the electric repulsive interaction among MPc molecules induced by the dipoles.

The void in the centre of the self-assembled hexamer structure is explained by steric constraint, *i.e.*, an additional molecule cannot be placed into the void, unless different surface sites for the terminal phenylene ring are assumed. With identical surface registry, phenylene hydrogens of the molecule in the centre would come too close to the phenylene hydrogens of the molecules in the wheel (Fig. 2b). Therefore, only the handed hexamer structure without a centre molecule is observed.

Based on different STM contrast observed in previous studies, different local geometries of the adsorbate complex have been proposed for SubPc.[20–22] In particular a bright protrusion in the centre has been assigned to a chlorine-up/bowl-opening-down configuration. For the molecules here, no bright protrusion is observed in STM at the centre of the three-spoke image, suggesting that the SubPc adsorbs on the Au(111) surface with the Cl atom pointing towards the substrate. In their report on SubPc on Ag(111), Berner *et al.* showed that the Cl atom faces the substrate and suggested that a partial charge transfer from the Ag substrate to the Cl of the SubPc leads to an induced interface dipole moment pointing towards the surface.[20] Here on Au(111), we expect a similar scenario with the charge transfer from Au *via* the chlorine to the SubPc molecule. However, despite this charge transfer, the Au–Cl bond seems to be relatively weak. That is, the zigzag herringbone stripes, which originate from the Au(111) reconstruction, are still present below the molecular islands (Fig. 1a) and imply that the reconstruction is not lifted upon adsorption of SubPc.

Diamond structure—high global coverage

With increasing coverage, the SubPc molecules form a 2D diamond-like pattern. Fig. 3a shows that the surface is almost completely covered by SubPc in form of ordered molecular islands. Higher magnification STM images (Fig. 3b and c) reveal that adjacent molecules directly face each other with two spokes, thus forming a diamond-like pattern. Like the honeycomb pattern at lower coverage, mirror domains are observed as well for this structure. The angle between the superlattice vectors of the molecular islands and the unit cell of Au(111) surface is $\pm 15^{\circ} \pm 1^{\circ}$, *i.e.*, identical with the honeycomb pattern within the error margins (see Fig. 3b). The relative arrangement of adjacent molecules, however, exhibits no handedness this time. Nevertheless, beyond the oblique angle between adlattice and substrate lattice, chiral expression is also present due to the relative azimuthal alignment of the molecules within the adsorbate unit cell. Even ignoring the substrate lattice, the two SubPc mirror unit cells can thus not be superimposed by rotation and translation within the plane. Typical examples for this kind of adsorption induced chirality are benzene superstructures on fcc(111) and hcp(0001) surfaces.[24]

Fig. 3d shows a structure model of the diamond structure. The relative orientation between adjacent molecules in the superlattice has changed. The nearest parts of two neighbouring molecules are phenylene rings facing directly each other without the set-off observed in the honeycomb pattern. The length of the adlattice vectors of the molecular unit cells is still 23 ± 1.0 Å (Fig. 3b and c), which gives the same packing density as the honeycomb structure. The unit cell habits are identical, but the relative arrangement of the two molecules has changed. This is quite remarkable, since the transition from honeycomb to diamond cannot be explained by closer packing. With increasing global coverage, a new arrangement with identical local density is established. One must keep in mind here that only certain sites, provided by the substrate lattice, and certain azimuthal orientations, due to the steric interaction between the molecules, are allowed. The transition between equally dense phases of bowl-shaped molecules with temperature has been accounted to an adsite change plus a size change due to ceasing bowl vibrations.[13] Here, however, the different phase is observed at the same temperature, but with increasing coverage. When the diamond structure nucleates and grows there are substantially more molecules on a single substrate terrace than in the case for the honeycomb formation. A limit in mobility could therefore impose a kinetic barrier, not allowing the final reorientation into a honeycomb pattern.

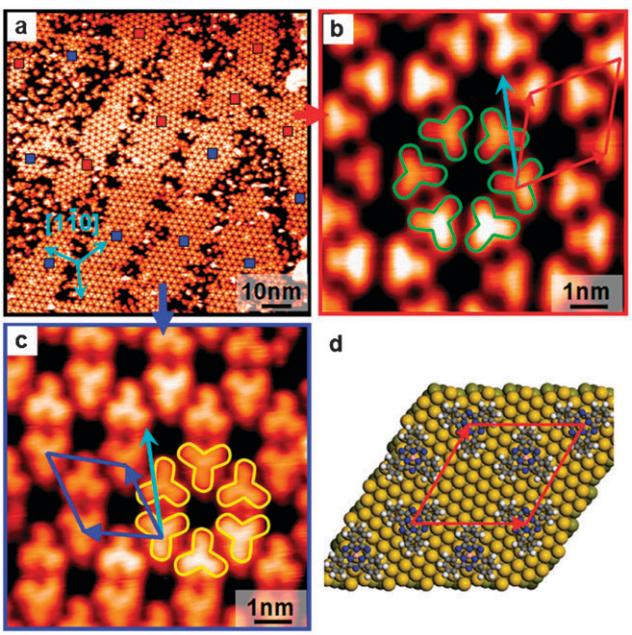

Fig. 3 (a) STM image (100 nm × 100 nm) of the diamond structure at high coverage, $V = -1.8$ V, $I = 0.08$ nA. Molecular mirror domains are coloured by red and blue squares. (b,c) High-resolution STM images (10 nm × 10 nm, $V = -1.4$ V, $I = 0.05$ nA) of right- and left-handed domains. The unit cells are indicated. (d) Structure model for the diamond structure.

Intermediate structure—high global coverage

Coexisting with the diamond phase, a similar structure is observed (Fig. 4). The basic building block consisting of the six SubPc molecules is identical, but the relative alignment of the six-molecule unit deviates from the diamond structure. That is, adjacent molecules of different 'diamond' hexamers are interlocked as in the honeycomb structure. This structure is therefore coined as 'intermediate' of 'honeycomb' and 'diamond' here. As a result, chirality is expressed again by a CW or CCW positioning of adjacent molecules, but this time at the level of hexamers. The local coverage, however, is slightly higher (Table 1). Intermediate and diamond are only found on separate terraces. Their coexistence must be explained as follows. Either local statistical coverage fluctuations favours nucleation of one phase, which then grows and dominates that terrace, or the intermediate structure nucleates and grows on the expense in coverage of other regions. At that temperature mass transport over step edges is still possible. Well-ordered and completely covered terraces by a single intermediate domain support this scenario (ESI†). This process has also been observed for a 2D-solid-state phase transition exhibiting a density change and mass transport over long distances.[13] Upon further cooling, the diamond phase nucleates on the other terraces with coverages below the critical value needed for intermediate phase nucleation. This mechanism is further supported by the fact that many domains exist on a single terrace. The boundaries cannot disappear and heal, because the temperature became too low. In that respect, 'diamond' and 'intermediate' must coexist and both structures are actually metastable transitional phases between the low-coverage honeycomb (ruled by attraction forces) and the saturation coverage hcp phase (ruled by repulsion forces, see explanation below). A similar phenomenon has been observed previously for helical aromatic molecules, where with increasing coverage an even lower density phase with a new relative azimuthal alignment of the molecules was established.[27]

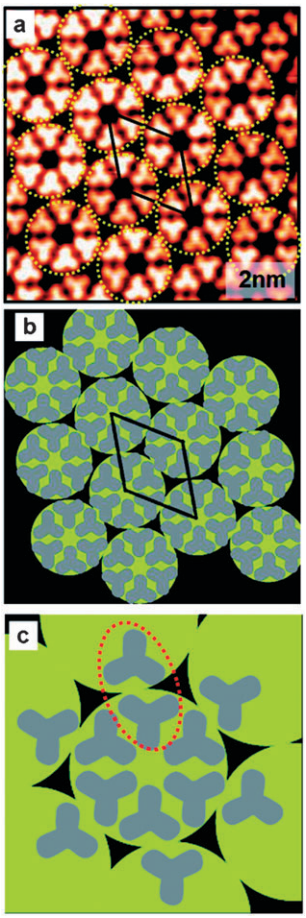

Fig. 4 (a) STM image (15 nm × 15 nm, $V = -1.8$ V, $I = 0.1$ nA) of a structure coexisting with the diamond structure at high coverage. The basic motif also a hexamer of SubPc molecules. (b) Schematic drawing of the STM image from (a). (c) Within a hexamer, the molecules show the face-to-face model as in the diamond pattern. Two neighbouring hexamers are relatively oriented with an offset (red dotted ellipse).

Hexagonal closed packed (hcp) structure—saturation coverage

When moving from one stable (or metastable) adsorption configuration to another, different kinetic barriers need to be overcome. It has been shown recently that a phase transition can be blocked just by confinement, not allowing the molecules to rearrange at all.[14] Here, the potential barriers increase as well with coverage. On one hand, the attractive interaction among SubPc molecules hampers the diffusion and the rearrangement of the SubPc molecules, on the other hand, however, the increasing density favours structures with lower repulsive terms in order to achieve more denser and closer-packed structures. The competition of these two interactions causes the limited movement and rotation of the adsorbate, and allows only the formation of 'intermediate' and 'diamond' at room temperature. However, if deposited at 380 K, the high mobility now allows formation of a well ordered monolayer with higher coverage (Fig. 5). The packing density increased substantially to 0.048 molecules per Au atom (Table 1). The driving force in lowering the overall energy is the gain in adsorption energy as long as the coverage can be increased. When the heat of adsorption per molecule becomes equal to the lateral repulsion, the saturation coverage is reached.[24]

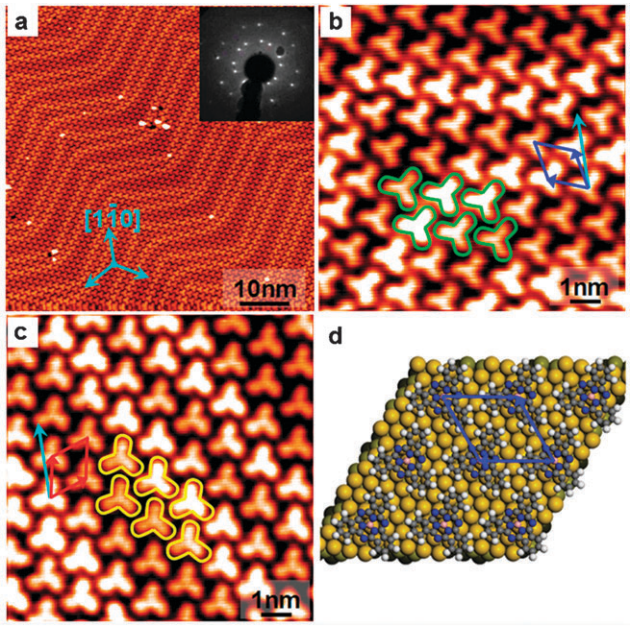

Fig. 5 (a) Large scale STM image of the well-ordered hcp layer (60 nm × 60 nm, $V = -2.0$ V, $I = 0.08$ nA). Cyan arrows indicate the $\langle 1\bar{1}0 \rangle$ substrate directions. The inset presents the LEED image taken with a beam energy 25 eV. (b), (c) Short-range STM images ($V = -2.0$ V, $I = 0.06$ nA). The enantiomorphous orientations of the molecular unit cells are identified by blue and red unit cells. The angle between the hcp lattice vectors and surface lattice vectors is $\theta_1 = -\theta_2 = 11^\circ \pm 1^\circ$. (d) Tentative model for the hcp structure.

The large-scale STM image and the corresponding LEED pattern of this structure reveal enantiomorphism again.

Table 1 Summary of structural parameters of observed phases. The experimentally installed global coverage is given as fraction of the densest monolayer available, *i.e.*, hcp ≡ 1 ML

Structure	Matrix notation	No. of unit cell molecules and substrate atoms	Angle w. r. t. [1$\bar{1}$0]	Local coverage in molec./Au atom	Global coverage/ML
Honeycomb	$\begin{pmatrix} 6 & -3 \\ 3 & 9 \end{pmatrix}$	2 molec. per 63	15°	0.032	0.2
Diamond	$\begin{pmatrix} 6 & -3 \\ 3 & 9 \end{pmatrix}$	2 molec. per 63	15°	0.032	0.6
Intermediate	$\begin{pmatrix} 13 & 0 \\ 0 & 13 \end{pmatrix}$	6 molec. per 169	0°	0.036	0.6
Hcp	$\begin{pmatrix} 4 & -1 \\ 1 & 5 \end{pmatrix}$	1 molec. per 21	11°	0.048	1.0

The angle between the two mirror domains (Fig. 5b and c) is approximately 22° ($\theta_1 = -\theta_2 = 11° \pm 1°$). Unlike the honeycomb pattern, two neighbouring molecules have the same orientation and self-organize into the 2D hexagonal close-packed (hcp) structure. The intermolecular distance is 13.5 ± 1.0 Å, which is also the length of the primitive lattice vectors of the hcp pattern unit cells. A model for the hcp structure is shown in Fig. 5d, the phenylene rings of SubPc molecule are pointing now to the notches of the adjacent molecules. In order to minimise repulsion, the hydrogen atoms of the phenylene rings are slightly interdigitated, instead facing directly each other. The latter has been suggested for SubPc molecules on Ag(111).[20]

Heating the sample does thermally activate the mobility and help molecules to self-organize into the most stable structure with high packing density. The different saturation structures for SubPc on Au(111) thus represents well the competition between kinetics and thermodynamics in 2D crystals. In particular it shows that the deposition conditions are crucial for these kind of studies. The remarkable square lattice, as previously reported for this SubPc/Au(111) system (C_{3v} molecule on a C_{3v} substrate),[22] must be assigned to the different deposition conditions. On Cu(100), a SubPc square structure has been reported as well.[21]

Conclusions

The growth of SubPc on a Au(111) single crystal surface was studied by means of STM. Depending on coverage, SubPc molecules are spontaneously oriented into ordered structures. Chirality is expressed at the supramolecular level in form of the relative alignment of substrate and adsorbate lattice, the relative alignment of molecular pairs, and the relative alignment of hexamers. At low coverage, island growth reveal attractive interactions. At higher coverage, metastable coexisting structures form, but the densest structure requires heating to overcome kinetic barriers. The polymorphism originates from the interplay of different intermolecular interactions during nucleation, *i.e.*, attraction *versus* repulsion, at different densities and the availability of preferred adsorption sites of the regular substrate. Although molecule and substrate possess identical C_{3v} symmetry, spontaneous symmetry breaking is observed.

Acknowledgements

We thank S. X. Du for fruitful discussion. This work was supported partially by the National Science Foundation of China (Grants 10674159 and 10874219) and the national 973 and 863 projects of China. KHE thanks the Swiss National Science Foundation and the Swiss State Secretariat for Education and Research (SER) for support.

References

1 B. Crone, A. Dodabalapur, Y.-Y. Lin, R. W. Filas, Z. Bao, A. LaDuca, R. Sarpeshkar, H. E. Katz and W. Li, *Nature*, 2000, **403**, 521.
2 S. R. Forrest, *Chem. Rev.*, 1997, **97**, 1793.
3 F. Zhao, F. Harnisch, U. Schröder, F. Scholz, P. Bogdanoff and I. Herrmann, *Electrochem. Commun.*, 2005, **7**, 1405.
4 C. Joachim, J. K. Gimzewski and A. Aviram, *Nature*, 2000, **408**, 541.
5 M. F. Cracium, S. Rogge and A. F. Morpurgo, *J. Am. Chem. Soc.*, 2005, **127**, 12210.
6 N. Papageorgiou, E. Salomon, T. Angot, J.-M. Layet, L. Giovanelli and G. L. Lay, *Prog. Surf. Sci.*, 2004, **77**, 139.
7 J. Hwang, A. Wan and A. Kahn, *Mater. Sci. Eng., R*, 2009, **64**, 1–31.
8 J. M. Gottfried and H. Marbach, *Z. Phys. Chem.*, 2009, **223**, 53.
9 M. Parschau, R. Fasel, K.-H. Ernst, O. Gröning, L. Brandenberger, R. Schillinger, T. Greber, A. Seitsonen, Y.-T. Wu and J. S. Siegel, *Angew. Chem., Int. Ed.*, 2007, **46**, 8258.
10 O. Guillermet, E. Niemi, S. Nagarajan, X. Bouju, D. Martrou, A. Gourdon and S. Gauthier, *Angew. Chem., Int. Ed.*, 2009, **48**, 1970.
11 T. Bauert, L. Merz, D. Bandera, M. Parschau, J. S. Siegel and K.-H. Ernst, *J. Am. Chem. Soc.*, 2009, **131**, 3460.
12 L. Merz, M. Parschau, J. S. Siegel and K.-H. Ernst, *Chimia*, 2009, **63**, 214.
13 L. Merz, M. Parschau, L. Zoppi, K. K. Baldridge, J. S. Siegel and K.-H. Ernst, *Angew. Chem., Int. Ed.*, 2009, **48**, 1966.
14 L. Merz, T. Bauert, M. Parschau, G. Koller, J. S. Siegel and K.-H. Ernst, *Chem. Commun.*, 2009, 5871.
15 W. Xiao, D. Passerone, P. Ruffieux, K. Ait-Mansour, O. Gröning, E. Tosatti, J. S. Siegel and R. Fasel, *J. Am. Chem. Soc.*, 2008, **130**, 4767.
16 H. Kietaibl, *Monatsh. Chem.*, 1974, **105**, 405.
17 A. Meller and A. Ossko, *Monatsh. Chem.*, 1972, **103**, 150.
18 H. Yanagi, D. Schlettwein, H. Nakayama and T. Nishino, *Phys. Rev. B: Condens. Matter Mater. Phys.*, 2000, **61**, 1959.
19 S. Berner, M. Brunner, L. Ramoino, H. Suzuki, H.-J. Güntherodt and T. A. Jung, *Chem. Phys. Lett.*, 2001, **348**, 175.
20 S. Berner, M. de Wild, L. Ramoino, S. Ivan, A. Baratoff, H.-J. Güntherodt, H. Suzuki and T. A. Jung, *Phys. Rev. B: Condens. Matter Mater. Phys.*, 2003, **68**, 115410.
21 H. Yanagi, K. Ikuta, H. Mukai and T. Shibutani, *Nano Lett.*, 2002, **2**, 951.
22 S. Mannsfeld, H. Reichhard and T. Fritz, *Surf. Sci.*, 2003, **525**, 215.
23 M. de Wild, S. Berner, H. Suzuki H. Yanagi, D. Schlettwein, S. Ivan, A. Baratoff, H.-J. Güntherodt and T. A. Jung, *ChemPhysChem*, 2002, **3**, 881.
24 K.-H. Ernst, *Top. Curr. Chem.*, 2006, **265**, 209.
25 Z. H. Cheng, L. Gao, Z. T. Deng, N. Jiang, Q. Liu, D. X. Shi, S. X. Du, H. M. Guo and H.-J. Gao, *J. Phys. Chem. C*, 2007, **111**, 9240.
26 C. Stadler, S. Hansen, I. Kröger, C. Kumpf and E. Umbach, *Nat. Phys.*, 2009, **5**, 153.
27 M. Parschau, R. Fasel and K.-H. Ernst, *Cryst. Growth Des.*, 2008, **8**, 1890.

